View metadata, citation and similar papers at core.ac.uk

brought to you by CORE

provided by Publications of the IAS Fellows

FEBS Journal

miR-22 regulates expression of oncogenic neuro-epithelial transforming gene 1, NET1

Hafiz M. Ahmad[1], Pamchui Muiwo[1], Suganthi S. Ramachandran[2], Priyatama Pandey[3], Yogendra K. Gupta[2], Lalit Kumar[4], Ritu Kulshreshtha[5] and Alok Bhattacharya[1]

1 School of Life Sciences, Jawaharlal Nehru University, New Delhi, India
2 Department of Pharmacology, All India Institute of Medical Sciences, New Delhi, India
3 School of Computational and Integrative Sciences, Jawaharlal Nehru University, New Delhi, India
4 Department of Medical Oncology, Institute Rotary Cancer Hospital, All India Institute of Medical Science, New Delhi, India
5 Department of Biochemical Engineering and Biotechnology, Indian Institute of Technology, New Delhi, India

Keywords
CD33$^+$; CML; HL60; K562; miR-22; NET1

Correspondence
A. Bhattacharya, School of Life Sciences, Jawaharlal Nehru University, New Delhi-110067, India
Fax: +91 11 2674 1586
Tel: +91 11 2670 4516
E-mail: alok.bhattacharya@gmail.com

(Received 15 January 2014, revised 17 May 2014, accepted 8 July 2014)

doi:10.1111/febs.12926

MicroRNAs control cellular processes by regulating expression of their target genes. Here we report that neuro-epithelial transforming gene 1 (NET1) is a target of tumor suppressor microRNA 22 (miR-22). miR-22 is downregulated in peripheral blood mononuclear cells derived from chronic myeloid leukemia (CML) patients and in CML cell line K562. NET1 was identified as one of the targets of miR-22 using both *in vitro* and *in vivo* experiments. Either mutations or naturally occurring single-nucleotide polymorphisms in NET1 3′-UTR that map at the miR-22 binding site were found to affect binding of miR-22 to NET1 mRNA. Over expression of NET1 in K562 cells resulted in increased proliferation. However decreased proliferation and alteration in cell cycle were observed on either overexpression of miR-22 or knockdown of NET1 expression respectively. We also found that overexpression of miR-22 or NET1 knockdown inhibits actin fiber formation, probably by downregulation of NET1 as NET1 knockdown also resulted in depletion of actin fiber formation. We suggest that the oncogenic properties of CML cells are probably due to deregulated expression of NET1 as a result of altered expression of miR-22.

Introduction

MicroRNAs (miRNAs) are small non-coding RNAs that have emerged as important regulatory factors involved in cellular decision making processes (for a recent review see [1]). They provide an additional layer of control at the post-transcriptional level and have been shown to be involved directly or indirectly in almost all physiological processes, most notably development, immune response and oncogenesis [2,3]. Mostly, miRNAs exert their regulatory effect by targeting cognate mRNAs through specific interaction with 3′-UTRs. Despite our understanding about some of the rules that govern miRNA–mRNA interaction, the problem of computational prediction of miRNA targets has not been completely solved. Available tools for target prediction display high levels of false positives and experimental validation is required for identification of targets. Since the biological basis of miRNA function is through modulation of targets, it is important to identify targets for functional characterization of miRNAs.

Chronic myelogenous leukemia (CML) is a myeloproliferative disorder of white blood cells characterized

Abbreviations
BrdU, 5-bromo-2-deoxyuridine; CML, chronic myelogenous leukemia; miR-22, microRNA 22; miRNA, microRNA; NET1, neuro-epithelial transforming gene 1; PBMC, peripheral blood mononuclear cell; PMA, phorbol 12-myristate 13-acetate; siRNA, small interfering RNA; SNP, single-nucleotide polymorphism.

by the presence of Philadelphia chromosome that is a result of a translocation event between the 9th and 22nd chromosomes [4]. The role of miRNAs in initiation, progression or treatment response of CML is not clear and there are only a few studies that link miRNAs with CML. miR-15 has been shown to regulate expression of c-MYB, thereby altering the proliferative properties of $CD34^+$ hematopoietic cells of CML patients [5]. miR-10a has also been implicated in CML as it is downregulated and its target upstream stimulatory factor 2 showed inverse expression with respect to miRNA level [6]. In the chronic phase, miR-17-92 cluster is upregulated. The expression of the cluster decreased with imatinib treatment similar to that seen after knockdown of BCR-ABL kinase gene [7]. On the other hand, miR-203 has been found to be a tumor suppressor as there was a reduction in both ABL/BCR-ABL level and proliferation of cells on its overexpression in CML cell line K562 [8]. miR-29b has also been shown to suppress CML cell proliferation [9]. Many miRNAs have been implicated in different types of cancers. However, their role in CML has not been studied. We carried out miRNA profiling of normal peripheral blood mononuclear cells (PBMCs), K562 and HL60 cells [10]. Our results suggested a generalized defect in miRNA production in K562 cells resulting in reduced levels of a number of miRNAs including miR-22. We observed downregulation of DICER1 in K562 cells [10]. Downregulation of DICER1 may be one of the reasons for reduction in miRNA level. miR-22 is thought to be a differentiation specific miRNA [11]. It is an important regulator of cardiac hypertrophy [12]. It is downregulated in gastric cancer and thought to be involved in invasion and migration [13]. A high miR-22 level is also known to suppress colon, ovarian and lung cancer progression and hypoxia signaling in colon cancer cells [14–17]. All these studies strongly indicate that miR-22 is a tumor suppressor, but its precise role and the mechanisms involved have not been addressed so far.

In the present study we have explored the role of miR-22 in CML and have identified one of the major targets of this miRNA. Our observations suggest a correlation between miR-22 level and the oncogenic status of cells. miR-22 is significantly downregulated in cells from CML patients, K562 and HL60 cells. We identified and validated NET1, a RhoA specific guanine nucleotide exchange factor, as one of the targets of miR-22. We also show that miR-22 has growth regulatory properties as it decreases proliferation of K562/HL60 cells, and this effect is mediated through NET1. It appears from our results that miR-22 participates in cancer cell biology by regulating NET1 expression.

Results

We had shown before that levels of a number miRNAs were considerably lower in a CML cell line K562 compared with normal PBMCs [10]. This may be an inherent property of CML cells or could be due to specific changes in K562 cells during the process of adaptation to become a cell line. If the former possibility is true then some of these miRNAs may have an important role in tumor formation. We have analyzed cells from CML patients and the results are shown below. It is also known that CML cells undergo differentiation to megakaryocytes in the presence of phorbol 12-myristate 13-acetate (PMA) [18]. The induced differentiated cells are thought to be a good model for normal cells and the dynamics of molecular changes can be studied easily using molecular tools in this system. Therefore, we have also used PMA-treated K562 cells in our attempt to understand the role of downregulation of miR-22 in CML.

miR-22 is downregulated in chronic myeloid leukemia cells

We estimated levels of a few selected miRNAs in PBMCs from CML patients and compared them with those of normal individuals. Initially qRT-PCR was used to quantify the levels of three miRNAs (miR-22, miR-27a and miR-324-5p) that displayed a low level of expression in K562 cells (Fig. 1A). These miRNAs are reported to have altered expression in several other malignancies, but so far there is no report that shows their involvement in CML [19–21]. The qRT-PCR results showed that the levels of miR-27a and miR-324-5p were also low in patients compared with normal individuals. However, the decrease was not as much as that seen for miR-22, being on average 80%, 44% and 51% for miR-22, miR-27a and miR-324-5p respectively (patient subset 1–5) (Fig. 1A). Therefore, further experiments were carried out only with respect to miR-22. In order to validate these results, we estimated the expression level of miR-22 in PBMCs of 25 more CML patients (patient subset 6–30). The results showed a consistent decrease in its expression ranging from 59% to 95% (on average 80% decrease) (Fig. 1B). Then we compared the expression of miR-22 in K562 relative to that in normal PBMCs. No significant amount of miR-22 was observed in K562 cells as expected, although PBMCs displayed a significant level of miR-22 (Fig. 1C). PBMCs are a mixed population of lymphoid and myeloid lineage cells where myeloid cells constitute approximately 50–85% of the total PBMCs [22]. In order to quantitate miR-22 expression

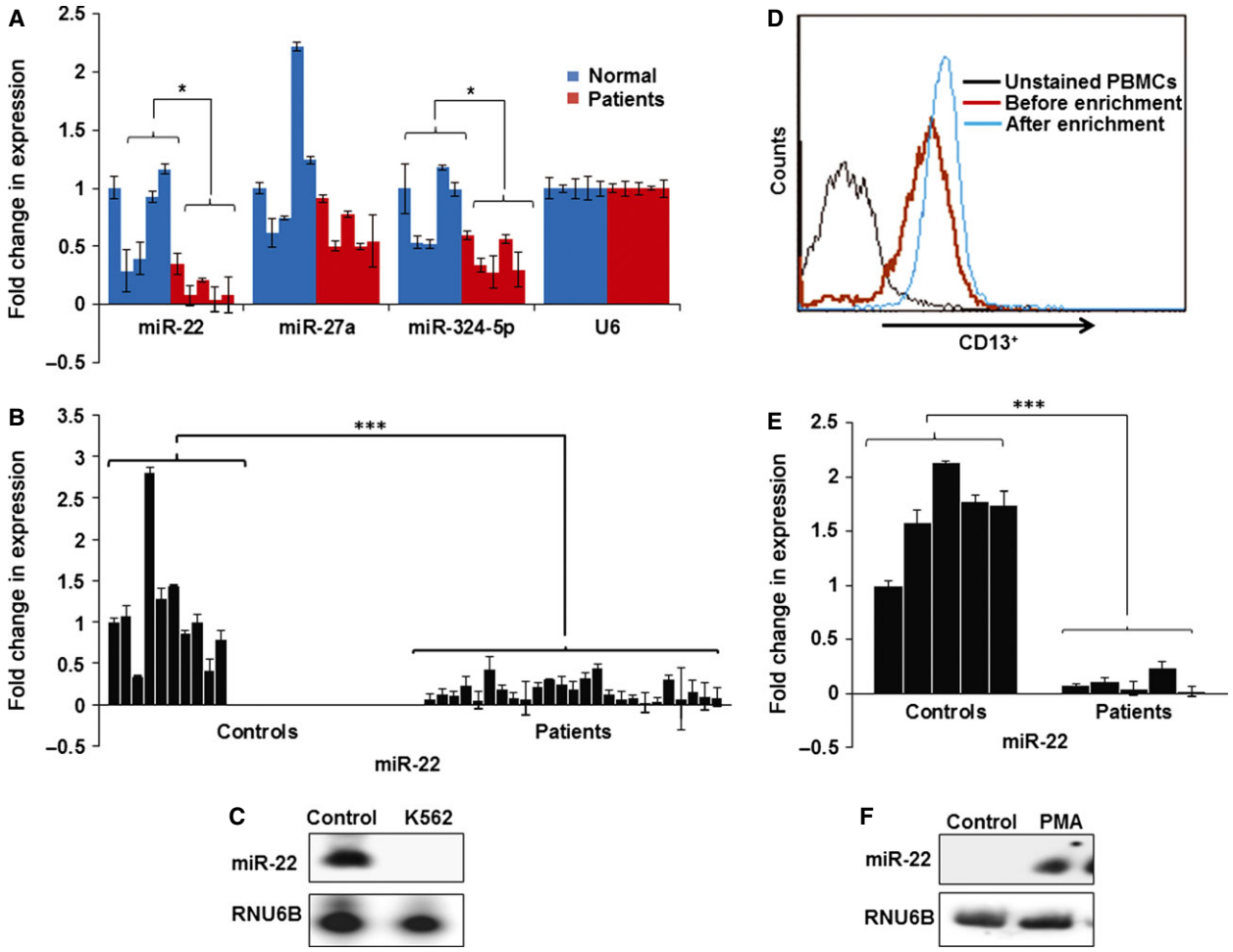

Fig. 1. miR-22 is downregulated in CML patients. Total RNA was extracted from indicated cells (PBMCs from CML patients, K562 cell line and PBMCs from normal individuals) following the standard protocol for analyzing miR-22 expression level. U6 RNA was used as a control. (A) Real-time PCR of miR-22, miR-27a and miR-324-5p (patient subset 1–5). (B) Real-time PCR of miR-22 in another set of patient samples (patient subset 6–30). (C) Northern blot of miR-22 of PBMCs/K562 cells using anti-miR-22 probe. (D) Flow cytometric analysis of enriched $CD33^+$ cells using IgG CD33 antibody coated magnetic beads. Analysis suggested 98% enrichment of $CD33^+$ cells. (E) qRT-PCR of miR-22 in $CD33^+$ enriched myeloid cells. (F) Northern blot of miR-22 after treatment of K562 cells with 20 nM PMA. miR-22 antisense DNA oligonucleotide was used as a probe for hybridization. Graphical data points denote mean ± SD (*t* test, $*P \leq 0.05$, $***P \leq 0.001$).

level in myeloid cells we further enriched the myeloid population by magnetic separation using IgG1 CD33 antibody conjugated with magnetic micro-beads. The CD33 cell surface marker is expressed on myeloid lineage cells but not on lymphoid cells [23]. We confirmed the purity of the separated myeloid cells by staining them with another myeloid specific marker CD13 [23]. The flow cytometry of CD13 stained cells suggested 98% final enrichment of myeloid cells (Fig. 1D). miR-22 expression was observed mainly in normal $CD33^+$ cells but not in $CD33^+$ cells from patient PBMCs suggesting that downregulation of miR-22 is a characteristic feature of leukemic myeloid cells (Fig. 1E).

A number of studies have shown that K562 can differentiate into megakaryocytes after treatment with PMA [18]. In order to check if miR-22 levels would also change on PMA treatment, northern blot analysis was carried out (Fig. 1F). The level of miR-22 increased by 85% upon PMA treatment while there was no change in the level of RNU6B RNA suggesting that miR-22 level is dependent on the differentiation status of cells.

NET1 is one of the targets of miR-22

miRNAs control cellular processes by binding and then regulating the levels and translation of their

target mRNAs [1]. In general there is a reciprocal relationship of miRNA levels with those of cognate mRNAs and the encoded polypeptides [1]. Usually miRNA targets can be predicted using a number of bioinformatics tools (for a recent review see [24]). It is recognized that target prediction tools quite often yield many false positive targets; therefore it is important that predictions are validated using experiments. Our prediction strategy involved integrating a web based target prediction program (MIRECORDS) and gene expression data from microarrays as described in Materials and methods. We found seven putative targets of miR-22 using the pipeline described here (Fig. 2A). A list of predicted targets is shown in Table 1. These putative targets were further substantiated by determining the expression of target genes and

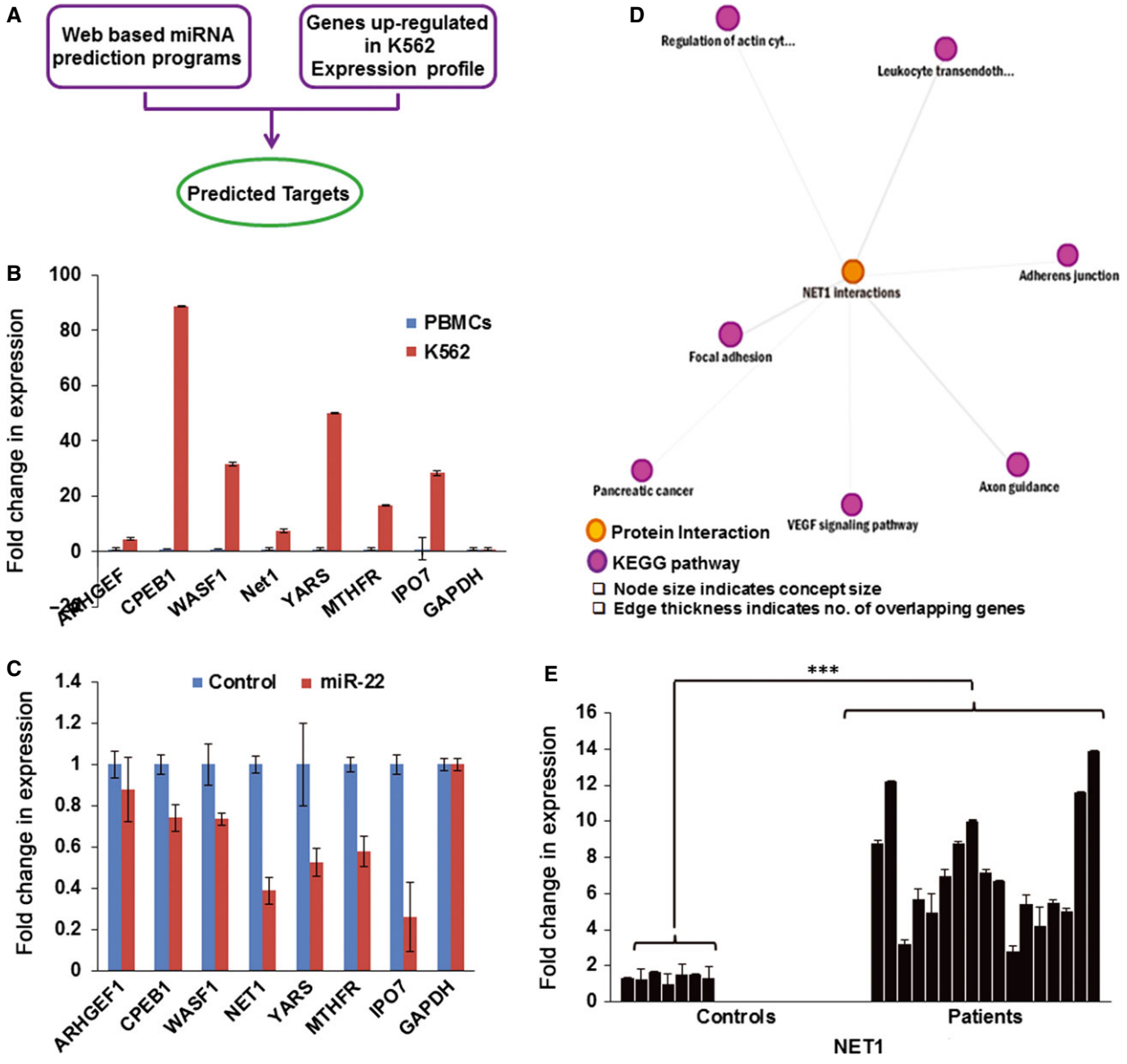

Fig. 2. Identification of miR-22 targets. (A) Targets of miR-22 were predicted using intersection of the online tool MIRECORDS and genes upregulated in K562 cells as identified by microarray experiments. The predicted targets are shown in Table 1. (B) qRT-PCR of indicated genes that were selected from Table 1. Data are represented as fold change in expression of K562 cells in comparison with normal PBMCs. (C) Expression level of some of the target genes after overexpression of miR-22. The controls were scrambled RNA expressing cells. (D) Gene function network for NET1 was generated by the online tool CONCEPTGEN. (E) qRT-PCR of NET1 in PBMCs of CML patients (patient subset 14–30). Graphical data points denote mean ± SD (*t* test, ***$P \leq 0.001$).

Table 1. Predicted target genes of miR-22.

ARHGEF
CPEB1
WASF1
NET1
YARS
MTHFR
IPO7

that of miRNAs. Levels of many predicted target genes, such as NET1, YARS and IPO7, displayed inverse correlation with that of miR-22 in normal PBMCs and K562 cells by real-time PCR (Fig. 2B). All putative targets showed a high level of expression in K562. In order to further confirm, miR-22 was overexpressed and the expression levels of different putative targets were determined. We expected that, on miR-22 overexpression, levels of real target genes would go down. The results showed that the levels of only two putative targets (NET1 and IPO7) were reduced significantly (Fig. 2C). All these results suggest that NET1 and IPO7 are likely to be the real targets of miR-22. We have carried out further experiments with NET1 as it is a RhoA specific guanine nucleotide exchange factor [25] and has been reported to be involved in pathways associated with actin cytoskeletal rearrangement, trans-endothelial migration of leucocytes, vascular endothelial growth factor signaling and pancreatic cancer (Fig. 2D) [26]. Further, we estimated the expression level of NET1 by qRT-PCR in PBMCs of CML patients (patient subset 14–30). The results showed that the level of NET1 was significantly higher in all the patients compared with that of the control cells validating the results obtained using cell lines (Fig. 2E). NET1 and miR-22 levels show an inverse correlation as expected if NET1 is one of the targets of miR-22. Analysis of expression data obtained from GEO suggested that the expression of NET1 is positively associated with many cancers, such as CML (GDS2342), prostate cancer (GDS1439), papillary thyroid carcinoma (GDS1732) and breast cancer (GDS1250). Furthermore, our analysis also showed that NET1 is expressed at a higher level in other myeloid leukemia cell lines, such as THP-1, KG-1 and U937 (GDS2251). In addition, we noticed that the level of NET1 is high in relapse cases in comparison with those where there is complete remission (GDS1059) (Fig. 3).

Further validation of NET1 as a target of miR-22 was done by using 3′-UTR reporter gene assay. Luciferase was used as a reporter and was cloned upstream of the 3′-UTR of NET1 so that luciferase level was controlled by miR-22. TARGETSCAN was used to identify the miR-22 binding site in NET1 3′-UTR (Fig. 4A). Mutant NET1 3′-UTR luciferase construct was generated where a mutation (three nucleotides at the fourth to sixth positions) was introduced at the miR-22 binding site, specifically in the seed binding region. While the level of luciferase decreased on overexpression of miR-22 when wild-type 3′-UTR was used, there was no significant change in luciferase expression when miR-22 was overexpressed in cells carrying mutant 3′-UTR luciferase construct (Fig. 4B). Similar observations were made when NET1 protein level was determined using western blotting. Overexpression of miR-22 decreased the level of NET1 (Fig. 4C) (Fig. 4D displays the expression level of transfected miR-22). We checked the specificity of interaction of miR-22 with NET1 by using full-length mutant NET1 carrying three altered nucleotides in the miRNA binding region. miR-22 was expressed in cells carrying mutant NET1. There was no effect of ectopically expressed miR-22 on mutant NET1 as no significant change in the level of NET1 was observed (Fig. 4E). The expression level of ectopically expressed miR-22 is also shown in Fig. 4F.

Single-nucleotide polymorphisms (SNPs) often modulate activities of genes, thereby regulating cellular physiology including tumorigenesis [27]. Therefore we searched for the presence of SNPs in 3′-UTR of NET1, particularly in the miR-22 recognition site, in order to identify genetic determinants that regulate miR-22 and NET1 interaction. The dbSNP was searched and 31 SNPs were found in the 3′-UTR of NET1. Amongst these, rs184456571 was mapped to the seed sequence of miR-22 binding site. In order to test if this SNP may have a physiological role we created a mutant NET1 3′-UTR containing the same change and used the luciferase reporter system for functional analysis. The results showed that the presence of this SNP is likely to generate an miR-22 insensitive form of NET1 (Fig. 4G). All these results suggest that NET1 is a validated target of miR-22 and that this SNP may have a role in regulating miR-22 mediated control of NET1 expression.

It has been mentioned that PMA differentiates K562 cells into megakaryocytes and consequently enhances the level of miR-22 in PMA-treated cells (Fig. 4H). Therefore it is expected that the NET1 level should go down after PMA treatment. Western blot analysis showed that the level of NET1 decreased significantly after treatment with PMA correlating with the increased expression of miR-22 (Fig. 4I). All these results strongly suggest that NET1 is one of the biologically relevant targets of miR-22.

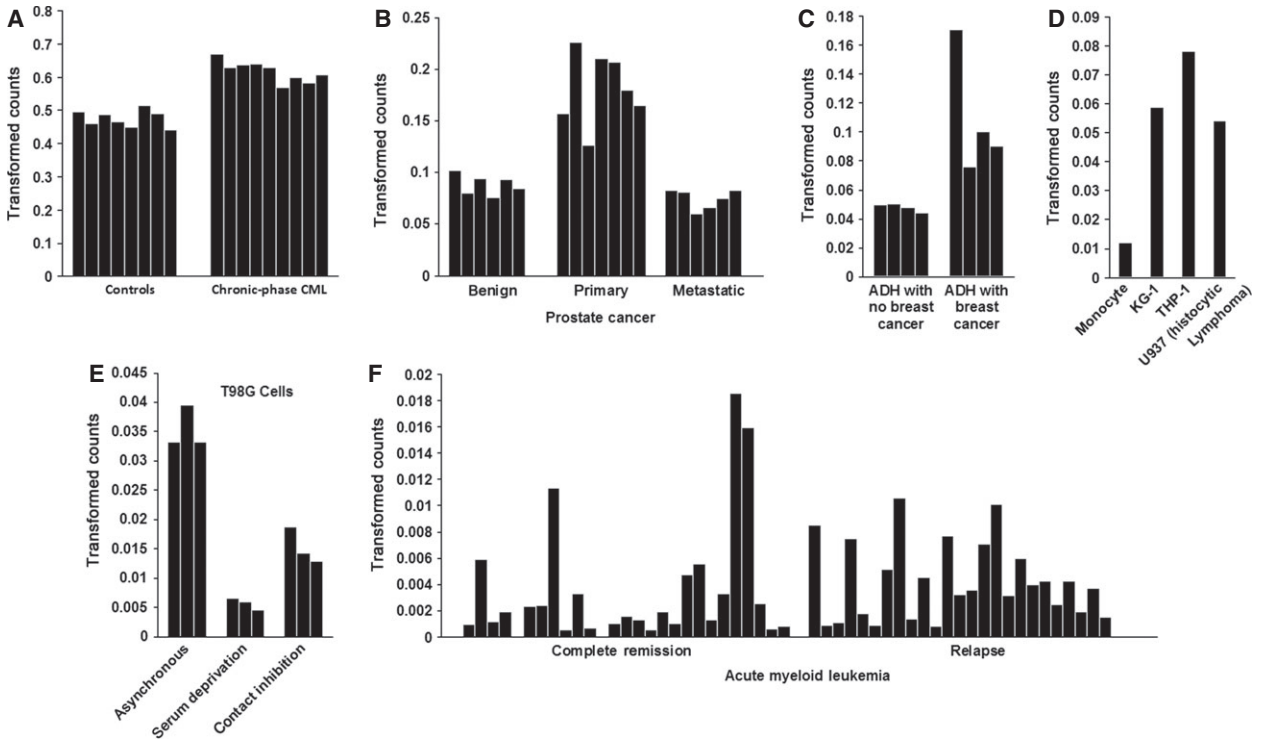

Fig. 3. GEO data analysis of NET1 expression in other cancers. (A) GDS2342: analysis of $CD34^+$ hematopoietic stem and progenitor cells from the bone marrow of untreated patients with CML in the first chronic phase. (B) GDS1439: expression level of NET1 in prostate cancer tumors that are benign, clinically localized, or metastatic and refractory to hormones. (C) GDS1250: comparison of atypical ductal hyperplasia (ADH) tissues from patients with and without a history of breast cancer. (D) GDS2251: comparison of myeloid leukemia cells with normal monocytes. (E) GDS911: expression level of NET1 in T98G cancer cells in growth arrest induced by 3 days of either serum deprivation or contact inhibition. (F) GDS1059: analysis of mononuclear cells from chemotherapy treated patients of <15 years of age with acute myeloid leukemia.

Analysis of miRNA and mRNA transcriptome of K562 cells treated with PMA

PMA-treated K562 cells differentiate into megakaryocytes and these treated cells are quite often used as a model for normal cells [28]. In order to find similarities in miRNA expression pattern between normal PBMCs and PMA-treated K562 cells we analyzed both miRNA as well as mRNA transcriptome of K562 cells with and without treatment with PMA. These results were compared with the results obtained when PBMCs from normal individuals were compared with K562. For miRNA transcriptome we carried out next generation sequencing of small RNAs and analyzed the results as described in our previous publication [10]. Expression of six miRNAs was found to follow the same pattern when either normal PBMCs or PMA-treated K562 cells were compared with untreated K562 cells (Table 2). Similarly we have looked at expression of putative targets of miR-22 and identified common differentially expressed target genes in K562 cells with or without PMA treatment and K562 cells relative to normal PBMCs. Targets which show inverse correlation with miR-22 upon PMA treatment (NET1, YARS, IPO7, WASF1 and CPEB1) were also observed in a K562/normal PBMC combination (Table 3). The results show that PMA-treated K562 cells partially behave like normal PBMCs and strengthen our earlier observation that NET1 is likely to be a major target of miR-22.

miR-22 is involved in cell growth and proliferation

NET1 has been suggested to be involved in proliferation and differentiation of myeloid cells [29]. Therefore we investigated the involvement of miR-22 in cellular proliferation. Upon overexpression of miR-22, the growth rate of K562 cells decreased by 50% compared with cells carrying a scramble control plasmid (Fig. 5A). When NET1 expression was downregulated by specific small interfering RNA (siRNA) in K562 cells, there was a decrease in cell proliferation by 43%. Correspondingly cell numbers increased by 42% on

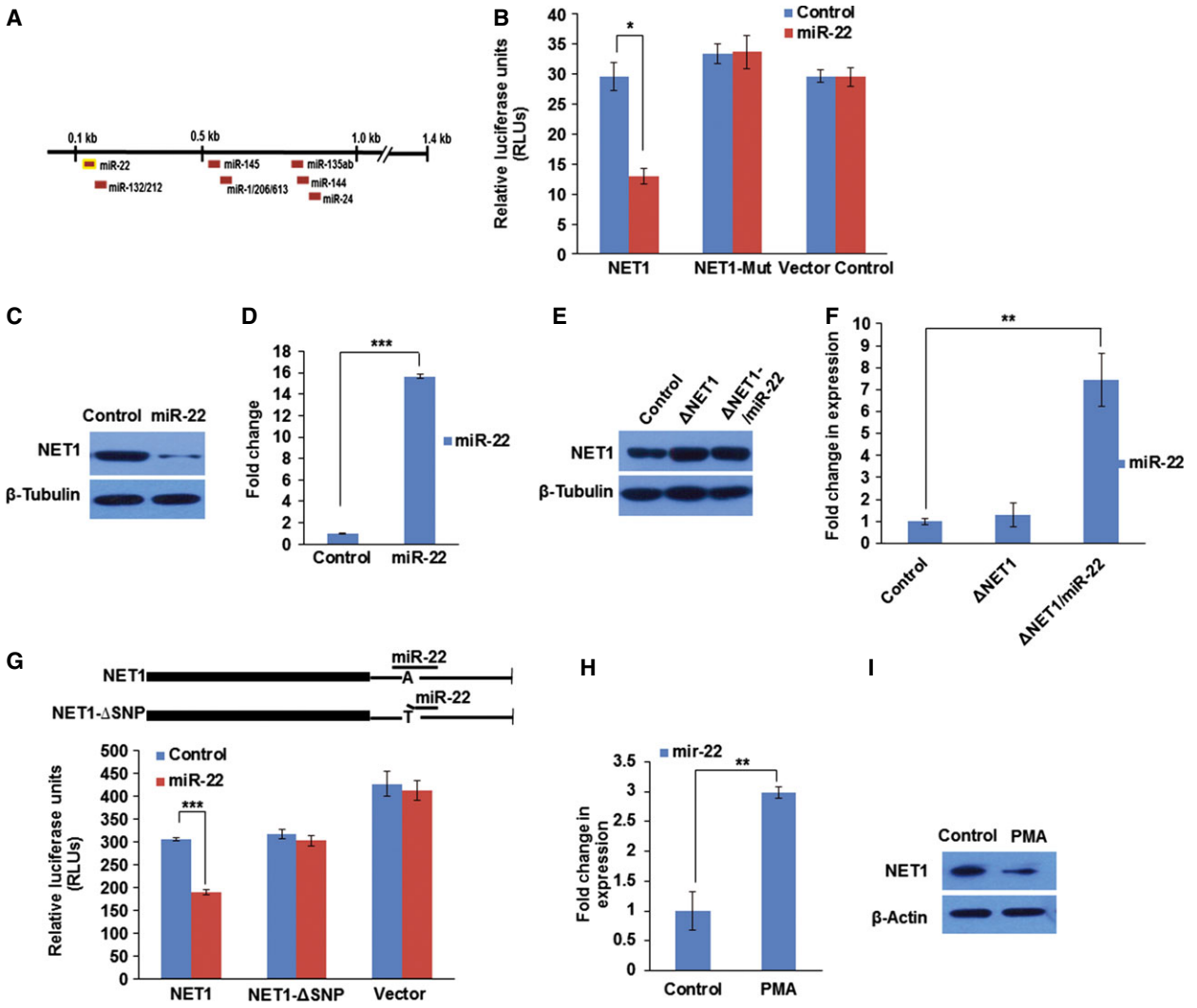

Fig. 4. miR-22 targets NET1. (A) Schematic representation of NET1 3′-UTR. It has one miR-22 binding site at the 5′ end. (B) Luciferase activity of constructs carrying wild-type and mutated NET1 3′-UTR in miR-22 overexpressing K562 cells. Mutation was carried out in the miR-22 complementary site. (C) Western blot of NET1 in miR-22 overexpressing K562 cells. (D) Graph represents the expression level of miR-22 in miR-22 overexpressed K562 cells. (E) Western blot of NET1 in K562 cells stably overexpressing mutated NET1 gene. The mutation was in the miR-22 binding site in the 3′-UTR. Mutant form of NET1 was transfected in K562 cells with or without miR-22. (F) Graph represents the expression level of miR-22. (G) The SNP (ID rs184456571) that maps to the miR-22 binding site of NET1 3′-UTR was identified by searching the dbSNP. Luciferase assay was carried out in cells carrying luciferase NET1 3′-UTR construct with or without miR-22 expressing plasmid. NET1 3′-UTR used here carried the SNP indicated above. (H) Expression level of miR-22 in PMA-treated K562 cells. (I) NET1 levels in K562 cells treated with 20 nM PMA were determined by western blot using IgG NET1 antibody. From (B) to (F) the controls were scrambled RNA expressing cells. Graphical data points denote mean ± SD (*t* test, $*P \leq 0.05$, $**P \leq 0.01$, $***P \leq 0.001$).

overexpression of NET1 (Fig. 5A). We also carried out a soft agar colony formation assay to assess the regulatory effect of transiently expressed miR-22 in K562 cells. We found that either overexpression of miR-22 or downregulation of NET1 expression by siRNA decreased drastically the number of K562 colonies (Fig. 5B). On the other hand overexpression of NET1 further enhanced colony formation (Fig. 5B). Colonies were counted with a Nikon SM2 1500 microscope. There was an approximately 0.50-fold decrease in the number of colonies in miR-22 overexpressing K562 cells (Fig. 5D). There was an increase in the number of colonies by more than 2-fold in NET1 overexpressed K562 cells (Fig. 5E) and a decrease of more than 0.30-fold in NET1 knocked down cells (Fig. 5F). The size of the colonies was also reduced in the case of miR-22 overexpression (average size of colonies became half, 60 257 μm^2 versus 136 773 μm^2,

Table 2. miRNAs displaying a similar expression pattern in normal PBMCs and PMA-differentiated K562 cells.

miRNA	Normal PBMCs/K562 cells (fold change)	PMA-treated K562/control K562 (fold change)
hsa-mir-146b	5.7057	2.3311074
hsa-mir-22	4.6518	2.0415248
hsa-mir-24	12.1140	3.7387884
hsa-mir-27a	11.802	2.9122117
hsa-mir-486	0.4135	0.3168723
hsa-mir-504	0.1125	0.3680543

Table 3. Expression of miR22 targets in PMA-treated K562 cells as deduced from microarray expression analysis.

Target genes of miR-22	Fold change ($\log_2$)
YARS	−1.64
NET1	−0.52
IPO7	−0.98
MTHFR	0.53
WASF1	−0.20
CPEB1	−0.42
ARHGEF12	0.01

$P \leq 0.005$) and NET1 knockdown (decreased by 0.63-fold, 35 430 μm^2 versus 55 584 μm^2, $P \leq 0.005$) as analyzed by NIS ELEMENTS AR 4.0 software. In NET1 overexpressed K562 cells, the size of the colonies increased significantly (3-fold, 81 464 μm^2 versus 27 270 μm^2, $P \leq 0.005$). When mutant NET1 (ΔNET1) was overexpressed there was no significant change in colony-forming units irrespective of whether miR-22 was overexpressed or not (Fig. 5C). Figure 5G shows the NET1 protein level in miR-22/NET1 overexpression and NET1 knockdown experiments. Figure 5H,I shows the expression level of ectopically expressed miR-22 in K562 cells used for the soft agar colony formation assay. Inhibition of proliferation was further analyzed to check if there is a block at a specific point in the cell cycle of K562 cells. There was a significant decrease (12.15%, $*P \leq 0.013$) at the G2/M phase of the cell cycle in cells overexpressing miR-22. A significant proportion of cells were arrested in the G1 (3.5%) and S phases (7%, $*P \leq 0.044$) (Fig. 5J). We also carried out cell cycle analysis after downregulation of NET1 expression with siRNA. The results were similar to that seen on overexpression of miR-22. After knockdown of NET1 there was a decrease of 10.28% ($**P \leq 0.0035$) at the G2/M phase with a concomitant increase of 11.50% ($***P \leq 0.0008$) in the G1 phase (Fig. 5K). On the other hand overexpression of NET1 increased the G2/M population of cells (8%, $*P \leq 0.019$) (Fig. 5L). In order to check whether the results may be due to decreased proliferation or cell death due to apoptosis, we performed 5-bromo-2-deoxyuridine (BrdU) incorporation assay in miR-22 overexpressed K562 cells. There was a 40% decrease in incorporation of BrdU in miR-22 overexpressed K562 cells suggesting that the decrease in the number of cells is indeed due to decreased proliferation of K562 cells (Fig. 5M). We can conclude from these results that miR-22 inhibits proliferation of K562 cells and this effect is probably due to targeting of NET1 by miR-22.

Effect of miR-22 on actin fiber formation

NET1 is known to modulate actin fiber formation as it regulates RhoA, a regulator of actin dynamics [30]. Therefore we checked the effect of ectopically expressed miR-22 on actin fiber formation. Overexpression of miR-22 in K562 cells decreased actin fiber formation as was evident from confocal microscopy images (Fig. 6A). The staining pattern was similar to that of cells where NET1 expression was downregulated with specific siRNA. The results

Fig. 5. Effect of miR-22 on growth and proliferation of K562 cells. (A) Proliferation was determined by measuring the number of cells at indicated times in cells stably expressing precursor miR-22 gene, NET1 and transiently expressed siNET1. The controls were scrambled RNA expressing cells. (B) Soft agar colony formation assay was also used as a measure of proliferation. It was carried out with K562 cells transiently expressing miR-22, NET1 or siRNA against NET1. The controls were scrambled RNA expressing cells. Colonies were counted on the 14th day. (C) Colony-forming units of cells overexpressing mutant NET1 (lacking miR-22 binding site) with or without overexpressed miR-22. Colonies were counted on the 14th day. The control was scrambled RNA expressing cells. (D–F) Graphs represent number of colonies in soft agar assay counted with the help of Nikon NIS ELEMENTS AR 4.0. (G) Western blots to show the level of NET1 in miR-22/NET1 overexpressed and NET1 knocked down cells using siRNA. (H–I) Graphs represent expression level of miR-22 in miR-22 overexpressed K562 cells used in the soft agar colony formation assay. Cell cycle analysis was carried out for indicated cells using flow cytometry after propidium iodide labeling following standard methods. (J) K562 cells overexpressing miR-22. (K) K562 cells transfected with siNET1. (L) K562 cells overexpressing NET1. All experiments were carried out three times. (M) BrdU uptake assay was performed to assess proliferation of stable miR-22 overexpressed K562 cells. Absorbance represents the extent of BrdU incorporated during the S phase of the cell cycle. Decrease in absorbance in miR-22 overexpressed cells suggests a decrease in proliferation of K562 cells. Graphical data points denote mean ± SD (*t* test, $*P \leq 0.05$, $**P \leq 0.01$, $***P \leq 0.001$).

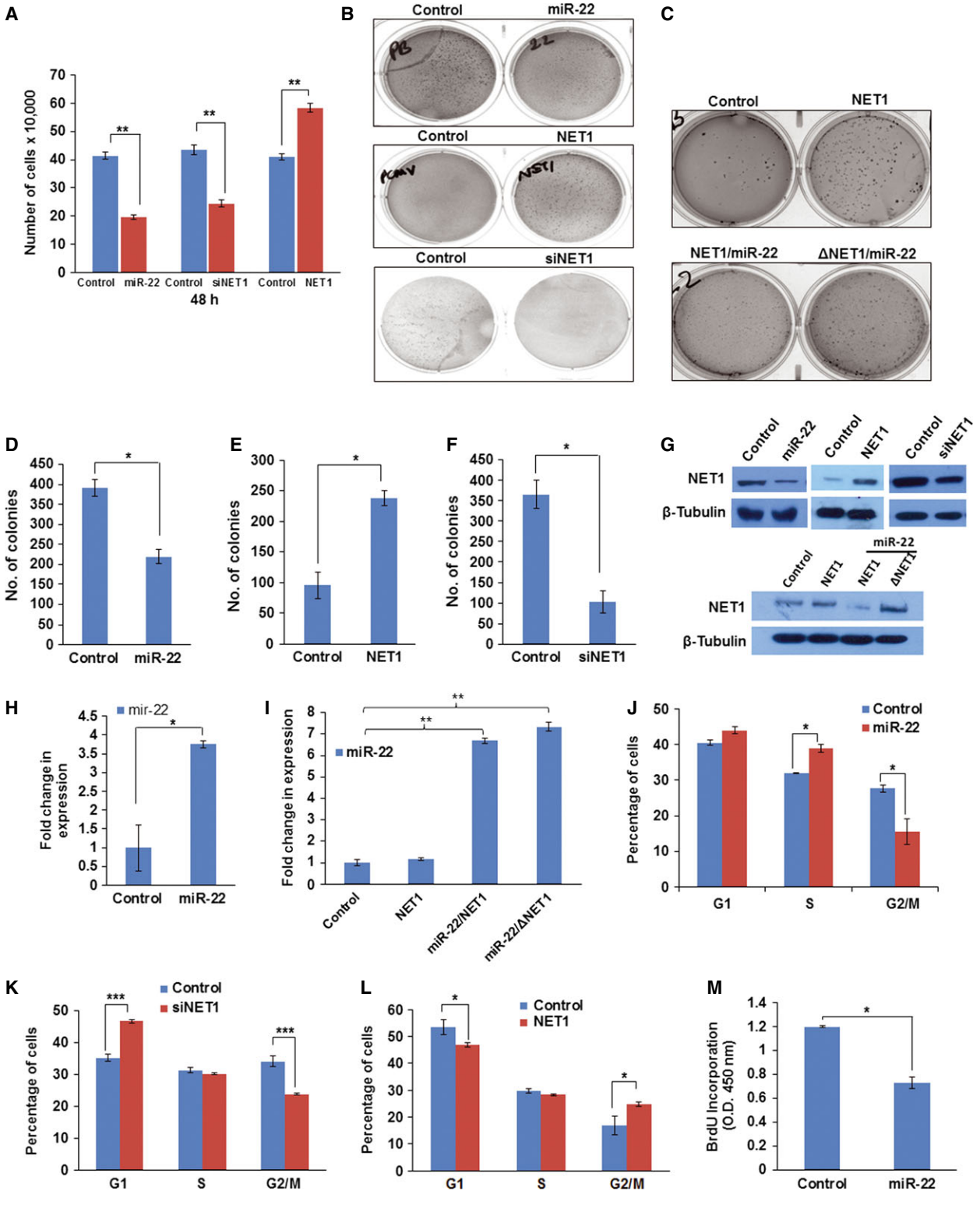

suggest that miR-22 may be regulating proliferation of cells by controlling actin dynamics. An intensity profile plot was generated on the basis of the intensity of actin fibers formed in the cytoplasm by IMAGEJ software using phalloidin. This was done by quantitatively analyzing the difference in actin fiber formation by

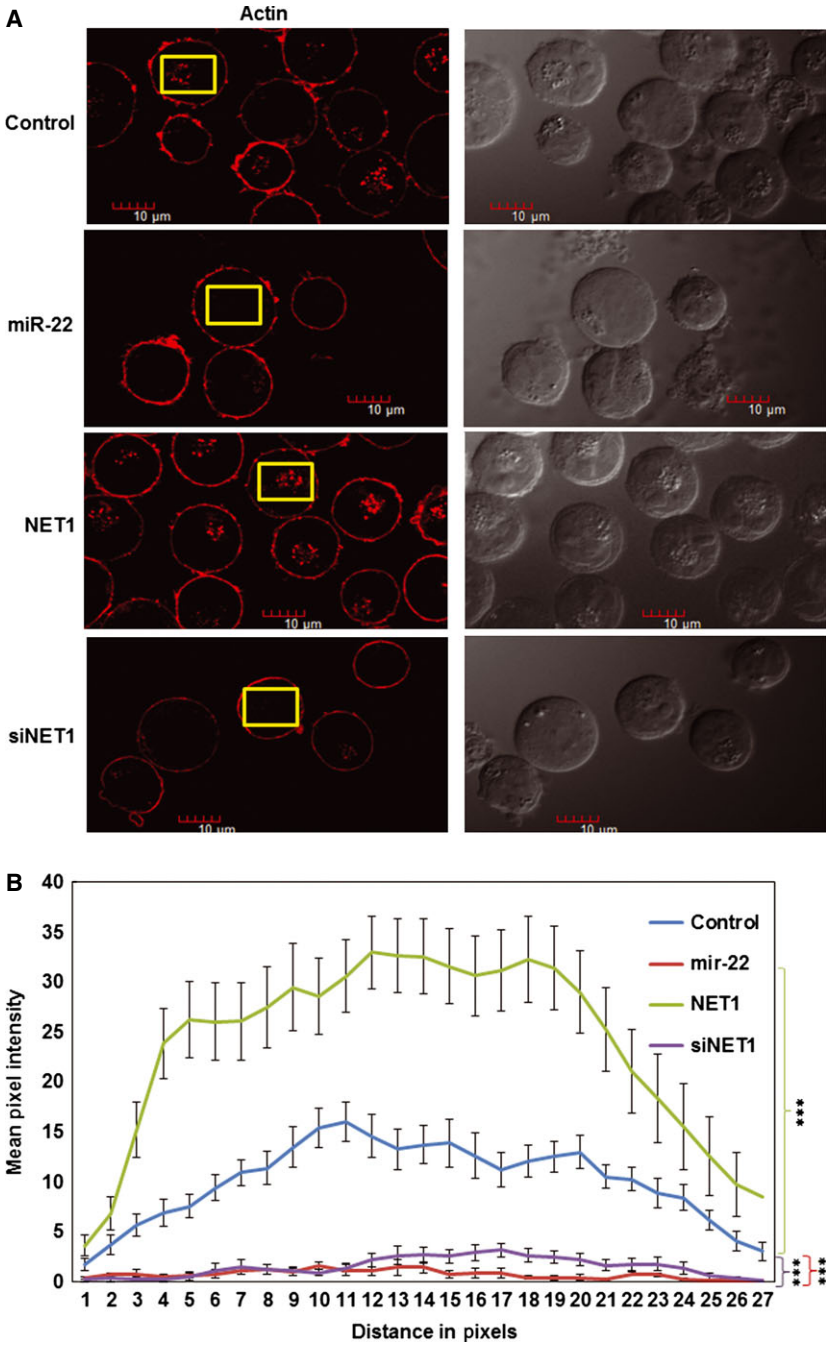

Fig. 6. Imaging of actin cytoskeleton in K562 cells. (A) Indicated cells were fixed and stained with phalloidin-TRITC before viewing under a confocal microscope (Olympus Fluoview FV1000). miR-22 and NET1 were transiently expressed in K562 cells. Imaging was also done with K562 cells containing siRNA against NET1 that resulted in low expression of NET1. (B) Intensity profiles represent the fluorescence intensity of actin stress fibers of the corresponding image. Graph represents the fluorescence intensity of actin in miR-22, NET1 and siRNA-NET1 transfected K562 cells. Data shown in the graph are an average of 15 randomly selected cells. Controls were scrambled RNA expressing cells. Graphical data points denote mean ± SEM. (*t* test, ***$P < 0.001$)

taking the average of 15 randomly selected cells from each experiment (miR-22 overexpressed, siNET1 and NET1 overexpressed cells) (Fig. 6B) [31]. The results showed that NET1 overexpression results in an increased amount of actin fiber formation. On the other hand the levels of actin fiber decreased on decreasing either NET1 expression or miR-22 overexpression (Fig. 6B).

In order to investigate whether the effect of miR-22 on NET1 expression is cell specific we have studied the effect of miR-22 on the proliferation of HL60 cells. These cells are derived from a patient with acute myeloid leukemia [32]. We had shown earlier that miR-22 is downregulated in HL60 cells [10]. We validated the low expression level of miR-22 in HL60 cells relative to that of normal PBMCs by qRT-PCR (Fig. 7A). When we overexpressed miR-22 in HL60 cells expression of NET1 decreased by 47% (Fig. 7B). miR-22 overexpressed HL60 cells displayed

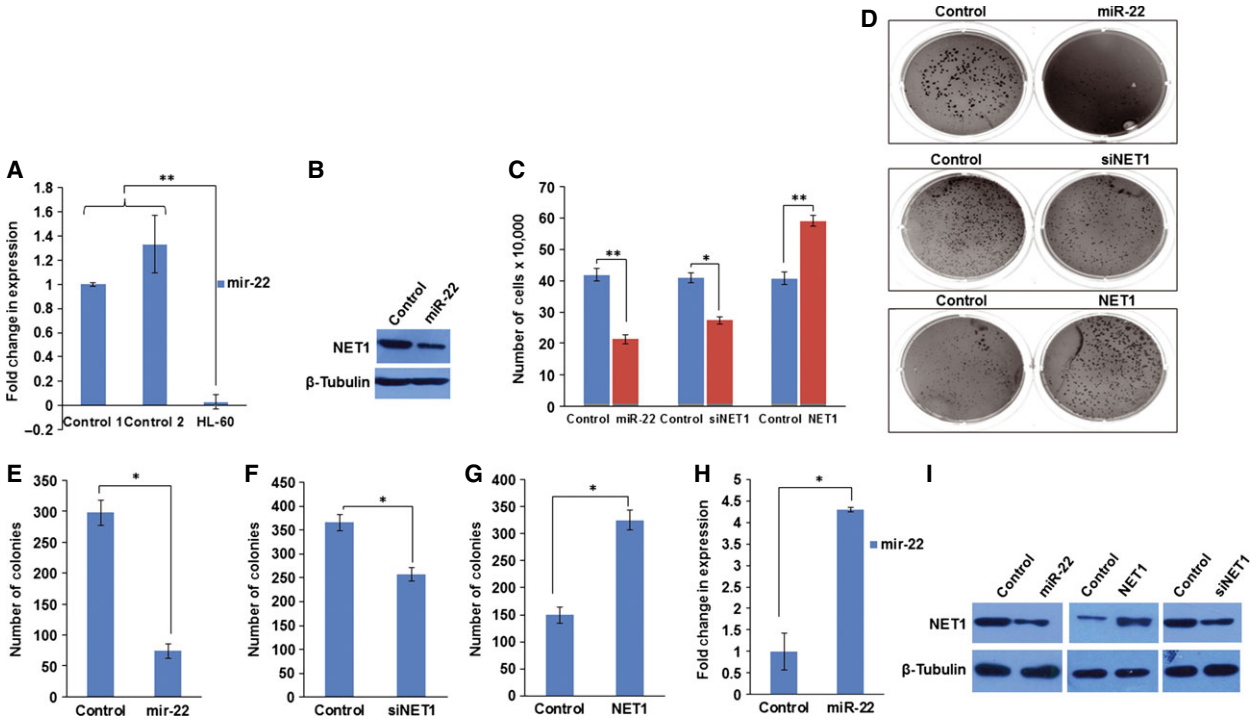

Fig. 7. Effect of miR-22 on proliferation of HL60 cells. (A) Graph represents the expression level of miR-22 in HL60 cells relative to PBMCs of two normal volunteers. (B) Expression level of NET1 in HL60 cells transiently overexpressing miR-22. (C) Proliferation was determined by measuring the number of HL60 cells that transiently overexpressed miR-22, NET and siRNA-NET1. The controls were scrambled RNA expressing cells. Cells were counted after 48 h. (D) Soft agar colony formation assay was carried out with HL60 cells transiently expressing miR-22, NET1 or siRNA against NET1. The controls were scrambled RNA expressing cells. Colonies were counted on the 14th day. (E–G) Graphs represent number of colonies in soft agar assays counted with the help of Nikon NIS ELEMENTS AR 4.0. (H) The graph represents the expression level of miR-22 in miR-22 overexpressed HL60 cells. Control cells were scrambled RNA expressing cells. (I) Western blot to show the level of NET1 in miR-22/NET1 overexpressed and NET1 knocked down cells. Graphical data points denote mean ± SD (*t* test, $*P \leq 0.05$, $**P \leq 0.01$).

a reduction in proliferation by 50%. Moreover, NET1 knockdown and NET1 overexpressed HL60 cells also showed altered proliferative ability, a reduction in growth by 35% and an increase in cellular proliferation by 45% respectively (Fig. 7C). We further performed soft agar colony formation assay to confirm the growth inhibitory effect of miR-22 in HL60 cells (Fig. 7D). miR-22 overexpressed cells exhibited a 0.25-fold decrease in colony number while NET1 knockdown and NET1 overexpressed HL60 cells showed a 0.75-fold decrease and a 2-fold increase in the number of colonies respectively (Fig. 7E,F,G). We also measured the size of the colonies. In the case of miR-22 overexpression, the colony size decreased (75 195 μm^2 versus 490 100 μm^2, $P \leq 0.0005$). In the case of NET1 knockdown the size of the colonies decreased (82 124 μm^2 versus 156 668 μm^2, $P \leq 0.005$) whereas there was an increase in colony size in NET1 overexpressed cells (485 527 μm^2 versus 136 162 μm^2, $P \leq 0.005$). Figure 7H shows the expression level of miR-22 in miR-22 overexpressed cells. Figure 7I shows the expression level of NET1 in miR-22 overexpressed, NET1 knockdown and NET1 overexpressed cells used in the soft agar colony formation assay. These results suggest that downregulation of miR-22 is an attribute of myeloid leukemia and is required for its regulated proliferation.

Discussion

miRNAs control gene expression at the post-transcriptional level, thereby bringing in an additional layer of control in gene regulation. Therefore, it is expected that any change in miRNA levels may result in alterations of the cellular state through regulation of gene networks resulting in initiation of the disease process [33]. A number of studies have already shown a linkage between altered levels of miRNAs and many diseases (for a recent review see [34]). Consequently it is not surprising that miRNAs may also be involved in the transition from normal to CML cells. We have shown earlier that there is a defect in miRNA synthe-

sis in the CML cell line K562 but not in the acute myeloid leukemia cell line HL60 [10]. Levels of a number of miRNAs were found to be significantly less in K562 cells compared with normal PBMCs. A number of miRNAs were also found to be downregulated in HL60 cells. In order to explore the relationship between low levels of some of the miRNAs and leukemia, we selected for further studies some of the low expressing miRNAs that are already suspected of participation in cancer. Estimation of expression level in 30 CML patient cells showed miR-22 to be the major downregulated miRNA among a few other miRNAs that were studied (miR-27a and miR-324-5p; these two miRNAs were studied in patient subset 1–5). This result along with the observations that overexpression of miR-22 altered the growth and proliferative property of K562 cells and that miR-22 levels increase on differentiation of these cells strongly indicated that it may be involved in leukemia genesis.

The results presented here clearly show that miR-22 mediates its biological function by targeting NET1. There are a number of reports that show that NET1 is a target of miR-22. For example, the complementary sequence of miR-22 is present in the 3′-UTR of NET1, expression of a reporter construct with NET1 3′-UTR is under the control of miR-22 levels and mutation of the complementary miR-22 recognition site abolishes this control by miR-22. Moreover, NET1 and miR-22 levels were inversely correlated when K562 cells were differentiated with PMA. NET1 has already been shown to be associated with cancer. It is known to be overexpressed in many malignancies and regulates invasion of cancerous cells [35,36]. However, the results presented here strongly indicate that NET1 is the main target that mediates the involvement of miR-22 in leukemia. We have observed that downregulation of NET1 gives the same phenotype as that seen on overexpression of miR-22 including reduction in the formation of actin fibers. Since NET1 is a regulator of RhoA that controls actin dynamics our results clearly indicate that some of the functions of miR-22 are mediated through NET1. miRNAs play a crucial role in regulation of NET1 expression during tumorigenesis as is evident by the finding that its expression is modulated by another miRNA miR-24 during epithelial to mesenchymal transition [37]. We also found that miR-24 is downregulated in K562 cells which suggests that regulation of NET1 expression in K562 cells may be the cumulative effect of miR-22 and miR-24. This is not surprising as it is known that on the one hand a number of miRNAs can target a single gene and on the other hand a single miRNA can target multiple genes [38]. Therefore miR-22 and NET1 along with other genes and miRNAs, such as miR-24, can form an intricate regulatory system, a perturbation of which can lead to tumor formation. Since miR-22 is likely to have other targets, it is possible that other targets may also be involved in mediating some of the functions of miR-22, e.g. miR-22 regulates Max expression and inhibits cell cycle progression in HL60 cells [11]. Recently, it has been reported that expression of miR-22 gets upregulated in myelo-dysplastic syndrome (MDS) [39]. In MDS miR-22 decreases the expression of its target gene TET2 that results in initiation and progression of MDS [39]. In our study, we found that TET2 expression is downregulated in the K562 (2.5-fold) and HL60 (0.8-fold) cell lines although the expression of miR-22 is also downregulated which suggests that other factors may be involved in the downregulation of TET2 in these cell lines. Our observation regarding the presence of an SNP in the miR-22 binding site of NET1 is intriguing. Although this SNP is thought to be rare, it appears to have a drastic effect in miR-22 regulation through NET1. At present we do not know the frequency of this SNP in the population nor do we have any idea of its biological role. However, we feel that a detailed analysis of the population may throw light on the importance of this SNP. In conclusion, we suggest that downregulation of miR-22 levels may have a crucial role in leukemia genesis and the transition to cancer cells may be partly mediated through NET1.

Materials and methods

Cell culture and reagents

K562 cell line was obtained from the National Centre for Cell Sciences, Pune, India and maintained in RPMI 1640 (Life Technologies, USA, cat no. 11875–119). The medium was supplemented with 10% fetal bovine serum (Life Technologies, USA, cat no 10082147) and penicillin–streptomycin and maintained at 37 °C with 5% CO_2 in an incubator chamber. HL60 cell line was a generous gift from S. Gopalan Sampathkumar, National Institute of Immunology, New Delhi, India. HL60 cells were grown in RPMI 1640 medium supplemented with 10% fetal bovine serum. PBMCs were obtained at the time of diagnosis from patients with CML after signed informed consent had been obtained from the patient in accordance with the Declaration of Helsinki. This study was approved by the hospital (AIIMS, New Delhi, India) according to the guidelines of the hospital's ethics committee (reference no. A-36:20/10/04). PMA (Sigma, USA, cat. no. P1585) treatment was given to K562 cells at a concentration of 20 nM. siNET1 (cat. no. 4392420, id: s20077) was purchased from Ambion, USA.

Cell separation

Myeloid cells were separated using Miltenyi Biotec magnetic cell sorting micro-beads with IgG CD33 antibody according to the manufacturer's protocol (cat. no. 130-045-501). Briefly, PBMCs were isolated by Histopaque (cat. no. 10771; Sigma) and approximately 10^7 cells were incubated with 20 μL IgG CD33 antibody conjugated with magnetic beads for 20 min. Cells were washed and passed through the column attached to a magnet. Cells were washed thrice and finally eluted. The purity of the separated cells was confirmed by staining them with FITC-CD13 antibody (cat. no. MHCD1301; Life Technologies) and analyzing by flow cytometry (FACSCalibur; BD).

RNA isolation and real-time PCR

Total RNA isolation was carried out from peripheral blood and K562 cells using TRIzol® Reagent (Invitrogen) as per the manufacturer's instruction. DNase 1 treatment was given to the total RNA as per the supplier's instruction (Invitrogen). Total RNA was used for cDNA synthesis using SuperscriptIII (Invitrogen). This cDNA was used for real-time PCR of miRNA target genes with SYBR Green chemistry (Applied Biosystems). Real-time PCR for miRNAs was performed with TaqMan miRNA assays according to the manufacturer's protocol (Applied Biosystems). Primers used for RT-PCR are as follows: F NET1, 5′-TGGTCACATTC TCGTGAGCTGGTTAC-3′; R NET1, 5′-CAATATAGC ATCCTCCAGAAGCTGAACATC-3′; F YARS, 5′-CCAG CTCAGCAAAGAGTACACACTAGATG-3′; R YARS, 5′-AATACTCTTCATCCAAAGCCTGCAGTC-3′; F MTHFR, 5′-CCGCTGGGGCAATTCCTCTTC- 3′; R MTHFR, 5′-CA GGCAAGTCACTTTGTGACCATTCC-3′; F IPO7, 5′-CA GCTCAATGAAGCACACAAGTCTCTG-3′; R IPO7, 5′-TG AATGCATGTAGTAAGCTGTACCCTGATG-3′; F GAP-DH, 5′-GGTCGGAGTCAACGGATTTGGTC-3′; R GAP-DH, 5′-GAGGGATCTCGCTCCTGGAAG-3′; F CPEB1, 5′-GAGCAGCACACACTCGGTACTGAG-3′; R CPEB1, 5′-GCGAAGGCTTGAAATCAAATCTGAG-3′; F ARHGE-F12, 5′-CACAGGCTCTGCTCAGGATGGA-3′; R ARHG-EF12, 5′-GGGCCACTCTTGGGACTATCTGC-3′; F WASF1, 5′-GAAGGAAAAGAGGAAGCAGAAGCA G-3′; R WASF1, 5′-CCACGTATGTCTGAGGTCTTGTT TC-3′.

Northern blotting

We did northern blotting for mature miRNA detection in PMA-treated K562 cells. The protocol used is a modification of the conventional northern blot developed by Pall *et al.* [40]. Here a chemical crosslinker, 1-ethyl-3-(3-dimethylaminopropyl) carbodiimide (EDC) (cat. no. E7750) is used instead of UV crosslinking. Briefly, 20 μg of total RNA was run on 15% denaturing urea PAGE. RNA was transferred to a nylon membrane and crosslinked by EDC for 1 h at 65 °C. The blot was probed with γP^{32}-end labeled antisense probe of miR-22 overnight at 42 °C. After washing, the blot was visualized using a Phosphorimager. The sequences of the antisense DNA probes for miR-22 and RNU6A were 5′-ACAGTTCTTCAACTGGCAGCTT-3′ and 5′-AATATG GAACGCTTCACGAATTTG-3′ respectively.

miRNA target prediction

The potential targets of the differentially regulated miRNAs were predicted using the following criteria. We used the online tool MIRECORDS for target prediction which uses an array of many target prediction programs (DIANA-MICROT, MICROINSPECTOR, MIRANDA, MIRTARGET2, MITARGET, NBMIRTAR, PICTAR, PITA, RNA22, RNAHYBRID and TARGETSCAN/TARGERTSCANS) [41]. We considered only those targets which were predicted by at least five programs. Then we compared these predicted targets with genes which were upregulated in K562 microarray data as we know miR-22 is downregulated in K562. Genes common in the prediction list and microarray data were selected as potential target candidates and were confirmed by experimental methods.

Western blotting

Total cell lysate was prepared in RIPA buffer. 50 μg of total cell lysate was used for western blotting. The lysate was run on SDS/PAGE and then transferred on a poly (vinylidene difluoride) membrane (Millipore, USA). The membrane was blocked in 5% BSA. The antibody for NET1 (cat. no. H00010276-B01) was purchased from Abnova and used according to the manufacturer's protocol. For loading control, we used β-actin/β-tubulin antibodies (BD Biosciences). Densitometry analysis was done using ALPHAIMAGER software.

Cloning and transfection

miR-22 was cloned in pBabe-puro vector by cloning a DNA fragment containing a sequence of miR-22 and its flanking region to make stable cell lines. 3′-UTR of NET1 was cloned downstream of the luciferase gene in pMIR-Report vector. Primers used for cloning were F NET1 5′-ATAGAGCTCGCTCTGTGTGTTAACTGATG GGAG-3′, R NET1 5′-ATAAAGCTTTATAATCGGGC TTTTACTCCTCCTC-3′. Mutant NET1 3′-UTR was generated by site directed mutagenesis. Primers used for mutagenesis were F NET1-mut 5′-GTTCTTTTTTCTTT TTTTAATGGGTCCTAAAGATATACAGATTACTG-3′, R NET1-mut 5′-CAGTAATCTGTATATCTTTAGGACC CATTAAAAAAAGAAAAAAGAAC-3′. Primers used for creating the SNP mutation in NET1 3′-UTR were F NET1-SNP 5′-GTTCTTTTTTCTTTTTTTAATGGCTGC

TAAAGATATACAGATTACTG-3′, R NET1-SNP 5′-AG TAATCTGTATATCTTTAGCAGCCATTAAAAAAAGA AAAAAGAAC-3′. Transfection of plasmids was done with Superfect (Qiagen). Transfection of pre-miR oligos was done with siPORT NeoFX transfection reagent (Ambion). Pre-miR-22 was used at a concentration of 30 nM. Transfection of siRNA was done with RNAiMax transfection reagent (Invitrogen) at a concentration of 10 nM.

Luciferase assay

Luciferase assay was performed with Dual Luciferase Assay Kit (Promega). For normalization we used PRL-TK vector. Cells were transfected with 3′-UTR containing luciferase vector in K562 cells with or without miR-22 and assayed after 48 h.

Growth assay

Growth assay was done with miR-22 overexpressing cell line. Cells were seeded in equal numbers for scramble vector control and miR-22 cell lines. Cells were manually counted after 24 and 48 h respectively.

Soft agar colony formation assay

Cells were transiently transfected with miR-22/NET1/siNET1 and then mixed with medium containing 0.70% agar (final concentration 0.35%) and poured on 1% base agar. Cells were allowed to grow for 10–15 days. Medium was changed every day. On the final day, cells were stained with 0.1% crystal violet and visualized under a Nikon SM2 1500 microscope. Further analysis of colony counting and colony size measurement was done with the help of NIS ELEMENTS AR 4.0 software.

Cell cycle analysis

Cell cycle analysis was done with propidium iodide staining. Briefly, cells were fixed in cold ethanol in 4 °C for 2 h. Then RNase treatment was given for 2 h by adding RNase at a final concentration of 250 $\mu g \cdot mL^{-1}$. After that propidium iodide was added at a final concentration of 50 $\mu g \cdot mL^{-1}$ for 20 min and cells were analyzed on a BD FACSCalibur instrument.

BrdU incorporation assay

BrdU incorporation assay was performed with BrdU cell proliferation assay kit (cat. no. 6813; Cell Signaling Technology) according to the manufacturer's protocol. Briefly, 4000 cells were plated in a 96-well plate. BrdU (20 μM) was added to the cells and these were incubated overnight at 37 °C. Cells were collected by centrifugation and were then treated with fixing/denaturing solution for 30 min before incubating with BrdU detection antibody for 1 h. Cells were incubated with horseradish peroxidase conjugated secondary antibody after washing for 30 min. The bound antibodies were then detected by incubating with TMB (3,3′,5,5′ TETRAMETHYLBENZIDINE) substrate for 30 min and the amount of color was determined at 450 nm using a plate reader.

Confocal microscopy

Cells were transiently transfected with miR-22/NET1/siNET1 and grown for 48 h. Cells were then transferred to a poly L-lysine treated coverslip for 1 h, washed with $NaCl/P_i$ and fixed with 3.7% paraformaldehyde for 30 min and washed again with $NaCl/P_i$. BSA (1% w/v) in $NaCl/P_i$ was used for blocking for 1 h; they were then stained with TRITC conjugated phalloidin for 30 min and washed with $NaCl/P_i$. Stained cells were mounted on a slide with DABCO and visualized using Olympus Fluoview FV1000 laser scanning microscope. An intensity profile plot was generated using IMAGEJ software [31].

Microarray analysis

Total RNA from normal PBMCs and K562 was used for microarray expression profiling as stated in our previous study and submitted in the GEO [10]. Microarray experiments were done with one normal PBMC sample and one K562 sample. The microarray for PMA-treated K562 was done on an Agilent platform (GEO accession no. GSE57734). Cells were treated with 20 nM PMA for 48 h and sent for microarray to Genotypic Technology, Bangalore. Analysis was done by GENESPRING GX version 12.0 software. The microarray of PMA-treated K562 cells was done with one control and one PMA-treated K562 cell sample.

miRNA transcriptome analysis

The miRNA expression profile was generated from next generation sequencing data as mentioned in our previous publication [42]. Briefly, reads from both samples were aligned to reference pre-miRNAs from miRBase release 20 and an expression profile of all isomirs was generated. All the isomirs were clustered by using specifically developed PERL script to give a complete expression profile.

Acknowledgements

HMA acknowledges Nishant Singh for his kind help in the flow cytometry experiments. We acknowledge Dr S. G. Sampathkumar for providing the HL60 cell line. We acknowledge JNU-AIRF and JNU-SLS-CIF for providing the confocal facility and flow cytometer respectively. AB thanks the Department of Biotechnology,

India (No. BT/PR1822/AGR/36/678/2011) and DST-JC Bose fellowship (No. SR/S2/JCB-51/2007) for funds. HMA thanks DBT for a fellowship (ref. no. DBT-JRF/07-08/280).

Author contributions

AB, RK and HMA conceptualized the project. AB and RK supervised the study. HMA did all the experimental work. LK and YKG conceptualized patient study and provided patient samples. PM and SSR carried out patient sample collection and RNA isolation from patient blood. PM did qRT-PCR of patient samples. PP did the next generation sequencing data analysis.

References

1 Yates LA, Norbury CJ & Gilbert RJ (2013) The long and short of microRNA. *Cell* **153**, 516–519.
2 Lujambio A & Lowe SW (2012) The microcosmos of cancer. *Nature* **482**, 347–355.
3 O'Connell RM, Rao DS, Chaudhuri AA & Baltimore D (2010) Physiological and pathological roles for microRNAs in the immune system. *Nat Rev Immunol* **10**, 111–122.
4 Maru Y (2012) Molecular biology of chronic myeloid leukemia. *Cancer Sci* **103**, 1601–1610.
5 Zhao H, Kalota A, Jin S & Gewirtz AM (2009) The c-myb proto-oncogene and microRNA-15a comprise an active autoregulatory feedback loop in human hematopoietic cells. *Blood* **113**, 505–516.
6 Agirre X, Jimenez-Velasco A, San Jose-Eneriz E, Garate L, Bandres E, Cordeu L, Aparicio O, Saez B, Navarro G, Vilas-Zornoza A *et al.* (2008) Down-regulation of hsa-miR-10a in chronic myeloid leukemia CD34+ cells increases USF2-mediated cell growth. *Mol Cancer Res* **6**, 1830–1840.
7 Venturini L, Battmer K, Castoldi M, Schultheis B, Hochhaus A, Muckenthaler MU, Ganser A, Eder M & Scherr M (2007) Expression of the miR-17-92 polycistron in chronic myeloid leukemia (CML) CD34+ cells. *Blood* **109**, 4399–4405.
8 Bueno MJ, de Perez Castro I, de Gomez Cedron M, Santos J, Calin GA, Cigudosa JC, Croce CM, Fernandez-Piqueras J & Malumbres M (2008) Genetic and epigenetic silencing of microRNA-203 enhances ABL1 and BCR-ABL1 oncogene expression. *Cancer Cell* **13**, 496–506.
9 Li Y, Wang H, Tao K, Xiao Q, Huang Z, Zhong L, Cao W, Wen J & Feng W (2013) miR-29b suppresses CML cell proliferation and induces apoptosis via regulation of BCR/ABL1 protein. *Exp Cell Res* **319**, 1094–1101.
10 Vaz C, Ahmad HM, Sharma P, Gupta R, Kumar L, Kulshreshtha R & Bhattacharya A (2010) Analysis of microRNA transcriptome by deep sequencing of small RNA libraries of peripheral blood. *BMC Genomics* **11**, 288.
11 Ting Y, Medina DJ, Strair RK & Schaar DG (2010) Differentiation-associated miR-22 represses Max expression and inhibits cell cycle progression. *Biochem Biophys Res Commun* **394**, 606–611.
12 Huang ZP, Chen J, Seok HY, Zhang Z, Kataoka M, Hu X & Wang DZ (2013) MicroRNA-22 regulates cardiac hypertrophy and remodeling in response to stress. *Circ Res* **112**, 1234–1243.
13 Guo MM, Hu LH, Wang YQ, Chen P, Huang JG, Lu N, He JH & Liao CG (2013) miR-22 is down-regulated in gastric cancer, and its overexpression inhibits cell migration and invasion via targeting transcription factor Sp1. *Med Oncol* **30**, 542.
14 Yamakuchi M, Yagi S, Ito T & Lowenstein CJ (2011) MicroRNA-22 regulates hypoxia signaling in colon cancer cells. *PLoS One* **6**, e20291.
15 Li B, Song Y, Liu TJ, Cui YB, Jiang Y, Xie ZS & Xie SL (2013) miRNA-22 suppresses colon cancer cell migration and invasion by inhibiting the expression of T-cell lymphoma invasion and metastasis 1 and matrix metalloproteinases 2 and 9. *Oncol Rep* **29**, 1932–1938.
16 Li J, Liang S, Jin H, Xu C, Ma D & Lu X (2012) Tiam1, negatively regulated by miR-22, miR-183 and miR-31, is involved in migration, invasion and viability of ovarian cancer cells. *Oncol Rep* **27**, 1835–1842.
17 Ling B, Wang GX, Long G, Qiu JH & Hu ZL (2012) Tumor suppressor miR-22 suppresses lung cancer cell progression through post-transcriptional regulation of ErbB3. *J Cancer Res Clin Oncol* **138**, 1355–1361.
18 Kang CD, Lee BK, Kim KW, Kim CM, Kim SH & Chung BS (1996) Signaling mechanism of PMA-induced differentiation of K562 cells. *Biochem Biophys Res Commun* **221**, 95–100.
19 Xu HS, Zong HL, Shang M, Ming X, Zhao JP, Ma C & Cao L (2014) miR-324-5p inhibits proliferation of glioma by target regulation of GLI1. *Eur Rev Med Pharmacol Sci* **18**, 828–832.
20 Scheibner KA, Teaboldt B, Hauer MC, Chen X, Cherukuri S, Guo Y, Kelley SM, Liu Z, Baer MR, Heimfeld S *et al.* (2012) miR-27a functions as a tumor suppressor in acute leukemia by regulating 14-3-3theta. *PLoS One* **7**, e50895.
21 Xiong J, Yu D, Wei N, Fu H, Cai T, Huang Y, Wu C, Zheng X, Du Q, Lin D *et al.* (2010) An estrogen receptor alpha suppressor, microRNA-22, is downregulated in estrogen receptor alpha-positive human breast cancer cell lines and clinical samples. *FEBS J* **277**, 1684–1694.
22 Feher JJ (2012) Quantitative Human Physiology: An Introduction. Elsevier, London.

23 Pearce DJ, Taussig DC & Bonnet D (2006) Implications of the expression of myeloid markers on normal and leukemic stem cells. *Cell Cycle* **5**, 271–273.
24 Zheng H, Fu R, Wang JT, Liu Q, Chen H & Jiang SW (2013) Advances in the techniques for the prediction of microRNA targets. *Int J Mol Sci* **14**, 8179–8187.
25 Alberts AS & Treisman R (1998) Activation of RhoA and SAPK/JNK signalling pathways by the RhoA-specific exchange factor mNET1. *EMBO J* **17**, 4075–4085.
26 Sartor MA, Mahavisno V, Keshamouni VG, Cavalcoli J, Wright Z, Karnovsky A, Kuick R, Jagadish HV, Mirel B, Weymouth T *et al.* (2010) ConceptGen: a gene set enrichment and gene set relation mapping tool. *Bioinformatics* **26**, 456–463.
27 Wong JC, Le Beau MM & Shannon K (2008) Tumor suppressor gene inactivation in myeloid malignancies. *Best Pract Res Clin Haematol* **21**, 601–614.
28 Shelly C, Petruzzelli L & Herrera R (1998) PMA-induced phenotypic changes in K562 cells: MAPK-dependent and -independent events. *Leukemia* **12**, 1951–1961.
29 Brazier H, Stephens S, Ory S, Fort P, Morrison N & Blangy A (2006) Expression profile of RhoGTPases and RhoGEFs during RANKL-stimulated osteoclastogenesis: identification of essential genes in osteoclasts. *J Bone Miner Res* **21**, 1387–1398.
30 Shen X, Li J, Hu PP, Waddell D, Zhang J & Wang XF (2001) The activity of guanine exchange factor NET1 is essential for transforming growth factor-beta-mediated stress fiber formation. *J Biol Chem* **276**, 15362–15368.
31 Schneider CA, Rasband WS & Eliceiri KW (2012) NIH Image to ImageJ: 25 years of image analysis. *Nat Methods* **9**, 671–675.
32 Gallagher R, Collins S, Trujillo J, McCredie K, Ahearn M, Tsai S, Metzgar R, Aulakh G, Ting R, Ruscetti F *et al.* (1979) Characterization of the continuous, differentiating myeloid cell line (HL-60) from a patient with acute promyelocytic leukemia. *Blood* **54**, 713–733.
33 Vaz C, Mer AS, Bhattacharya A & Ramaswamy R (2011) MicroRNAs modulate the dynamics of the NF-kappaB signaling pathway. *PLoS One* **6**, e27774.
34 Mo YY (2012) MicroRNA regulatory networks and human disease. *Cell Mol Life Sci* **69**, 3529–3531.
35 Bennett G, Sadlier D, Doran PP, Macmathuna P & Murray DW (2011) A functional and transcriptomic analysis of NET1 bioactivity in gastric cancer. *BMC Cancer* **11**, 50.
36 Carr HS, Zuo Y, Oh W & Frost JA (2013) Regulation of FAK activation, breast cancer cell motility and amoeboid invasion by the RhoA GEF Net1. *Mol Cell Biol* **33**, 2773–2786.
37 Papadimitriou E, Vasilaki E, Vorvis C, Iliopoulos D, Moustakas A, Kardassis D & Stournaras C (2012) Differential regulation of the two RhoA-specific GEF isoforms Net1/Net1A by TGF-beta and miR-24: role in epithelial-to-mesenchymal transition. *Oncogene* **31**, 2862–2875.
38 Hashimoto Y, Akiyama Y & Yuasa Y (2013) Multiple-to-multiple relationships between microRNAs and target genes in gastric cancer. *PLoS One* **8**, e62589.
39 Song SJ, Ito K, Ala U, Kats L, Webster K, Sun SM, Jongen-Lavrencic M, Manova-Todorova K, Teruya-Feldstein J, Avigan DE *et al.* (2013) The oncogenic microRNA miR-22 targets the TET2 tumor suppressor to promote hematopoietic stem cell self-renewal and transformation. *Cell Stem Cell* **13**, 87–101.
40 Pall GS & Hamilton AJ (2008) Improved northern blot method for enhanced detection of small RNA. *Nat Protoc* **3**, 1077–1084.
41 Xiao F, Zuo Z, Cai G, Kang S, Gao X & Li T (2009) miRecords: an integrated resource for microRNA-target interactions. *Nucleic Acids Res* **37**, D105–D110.
42 Vaz C, Ahmad HM, Bharti R, Pandey P, Kumar L, Kulshreshtha R & Bhattacharya A (2013) Analysis of the microRNA transcriptome and expression of different isomiRs in human peripheral blood mononuclear cells. *BMC Res Notes* **6**, 390.